Electronic Supplementary Material (ESI) for Soft Matter.

Supporting Information

for

Mutualistic benefit in the self-sorted co-aggregates of *peri*-naphthoindigo and a 4-amino-1,8-naphthalmide derivative

*Rashmi Jyoti Das and Kingsuk Mahata**

Department of Chemistry, Indian Institute of Technology Guwahati, Guwahati -781039, India
E-mail: kingsuk@iitg.ac.in
Fax: (+91) 361-258-2349

Table of contents

1. Materials and methods

Deuterated solvents (DMSO-d_6: 99.9 atom % D; C_6D_6: 99.6 atom % D) and potassium bromide (FT-IR grade) were procured from Sigma Aldrich. HPLC and UV grade solvents were purchased from either Merck or Spectrochem. ^{1}H and ^{13}C NMR measurements were done at 295 K on either Bruker AscendTM 400 MHz NMR spectrometer or Bruker Avance III 600 MHz NMR spectrometer using deuterated solvent as the lock and residual solvent as the internal reference. Chemical shifts are reported in δ (ppm) relative to the residual solvent peak (DMSO-d_6: 2.50 for ^{1}H, 39.43 for ^{13}C; C_6D_6: 7.15 for ^{1}H). The following abbreviations were utilised to describe peak patterns: s = singlet, d = doublet, dd = doublet of doublet, t = triplet and m = multiplet. High resolution mass spectrometry (HRMS) measurements were done with Agilent QTOF 6520 mass spectrometer using electrospray ionization (ESI) mode. Infra-red (IR) spectra were collected as a film on KBr using Perkin-Elmer FT-IR spectrometer and frequencies are presented in reciprocal centimeter (cm^{-1}). UV-vis absorption measurements were carried out on Perkin-Elmer Lamda-25, Lambda-35 and Lamda-750 spectrophotometer at 293 K. Depending upon concentrations, samples were loaded either in 1 mm or in 10 mm path length quartz UV-cuvette. Photoluminescence (PL) spectra were recorded on a Horiba Fluoromax-4 spectrofluorometer. A 10 mm × 10 mm quartz cuvette was used for the solution spectra at 293 K. The spectra were corrected using the correction factor implemented in the software. The time-resolved fluorescence was recorded in a time-correlated single photon counting (TCSPC) setup (Horiba Instruments) using a picosecond laser diode (Horiba Instruments) of 405 nm excitation wavelength. FWHM of the setup was typically ~90 ps. The fluorescence decays were fitted using DAS6 software (Horiba Instruments). The fluorescence transients were recorded by keeping the analyzer at the magic angle (55^o) with respect to the polarizer. FESEM images were recorded either on Sigma 300 or Gemini 300 microscope. Samples were made by drop-cast method from the respective solvent system and were left for drying at room temperature. Powder X-ray diffraction patterns were measured on a Rigaku Smartlab X-ray diffractometer.

Compound PNI,[1] H-NMI,[2] and NH_2-NMI[3] were prepared according to known procedures. However, analytical data of NH_2-NMI was not reported. Complete characterization data of NH_2-NMI is described below.

2. Synthesis of NH_2-NMI

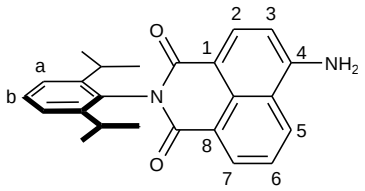

NH_2-NMI

NH_2-NMI was prepared from 4-nitro-1,8-naphthalic anhydride in a two-step procedure.

Step 1: To a suspension of 4-nitro-1,8-naphthalic anhydride (1.50 g, 7.04 mmol) in 10 mL of acetic acid, 2,6-diisopropyl aniline (2.21 mL, 10.55 mmol) was added. The reaction mixture was heated at 110°C for 24 h. It was then terminated by addition of ice-water. The product was extracted with ethyl acetate (3 x 30 mL), washed with brine and deionised water. The combined organic layer was dried over anhydrous sodium sulfate and filtered. After evaporating the solvent, the residue was purified by column chromatography using 10% ethyl acetate in hexane as eluent. NO_2-NMI was isolated as yellow solid and used for the next step. Yield: 850 mg (56.7%).

Step 2: To a mixture of NO_2-NMI (550 mg, 1.37 mmol) and $SnCl_2.2H_2O$ (1.54 g, 6.83 mmol) in ethanol (15 mL) was added 0.10 mL of HCl (36%). The reaction mixture was refluxed for 18 h. Upon cooling a yellow precipitate was obtained. The resulting product was filtered out, washed with aqueous Na_2CO_3 and dried under vacuum to obtain the NH_2-NMI as light-yellow solid. Yield: 360 mg (71%). ^{1}H NMR (600 MHz, DMSO-d_6) δ 1.03-1.04 (m, 12H, methyl-H), 2.60 (m, 2H, C-H), 6.89 (d, ^3J = 8.4 Hz 1H, 3-H), 7.28 (d, ^3J = 7.8 Hz, 2H, a-H), 7.40 (t, ^3J = 7.8 Hz, 1H, b-H), 7.60 (s, 2H, N-H), 7.69 (dd, ^3J = 8.2 Hz, ^3J = 7.6 Hz, 1H, 6-H), 8.23 (d, ^3J = 8.4 Hz, 1H, 2-H) 8.47 (d, ^3J = 7.6 Hz, 1H, 5-H), 8.70 (d, ^3J = 8.2 Hz, 1H, 7-H) ppm; ^{13}C NMR (150 MHz, DMSO-d_6) δ 23.5, 28.4, 107.1, 108.3, 119.5, 121.6, 123.4, 124.1, 128.6, 129.8, 130.3, 131.5, 131.9, 134.4, 145.3, 153.1, 163.1, 164.1 ppm; HRMS (ESI) m/z calcd for $[C_{24}H_{24}N_2O_2 + H]^+$ 373.1915, found: 373.1955; UV/vis (THF) λ_{max}/nm (ε/$M^{-1}cm^{-1}$) 419 (22 440).

3. NMR spectra

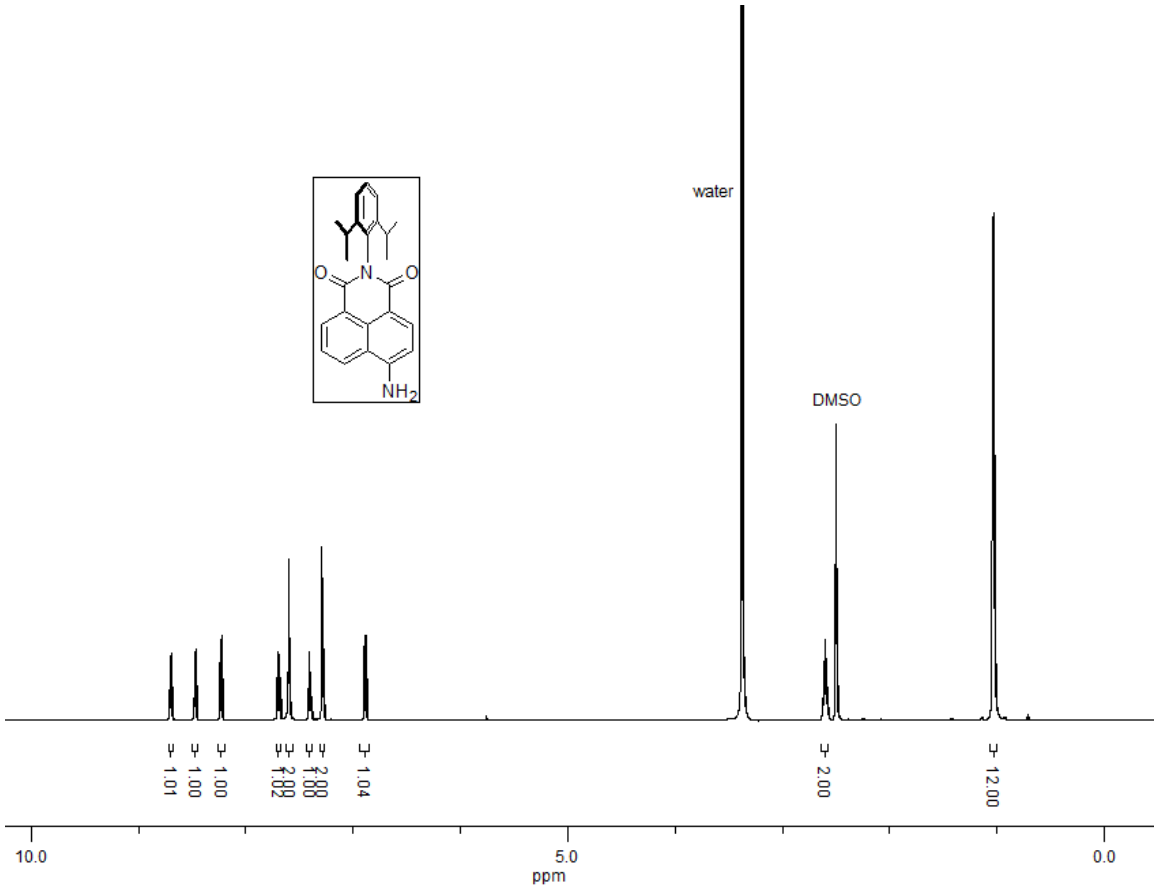

Fig. S1 ^{1}H NMR spectrum of NH_2-NMI (600 MHz, DMSO-d_6, 295 K).

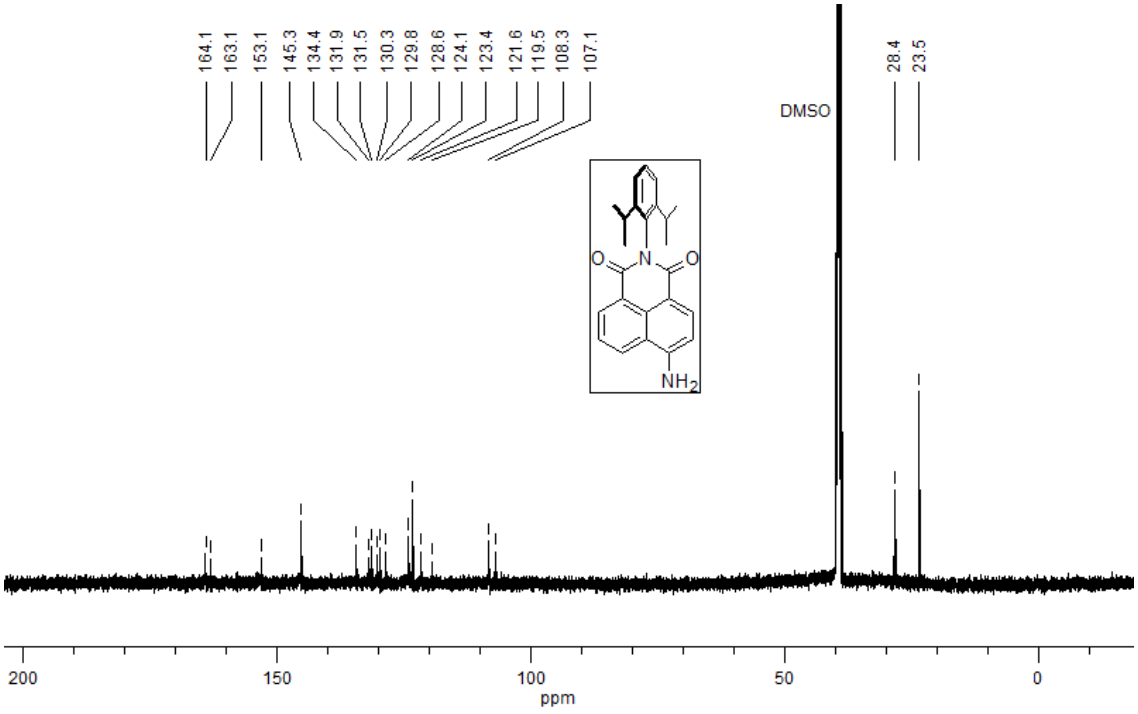

Fig. S2 ^{13}C NMR spectrum of NH_2-NMI (150 MHz, DMSO-d_6), 295 K.

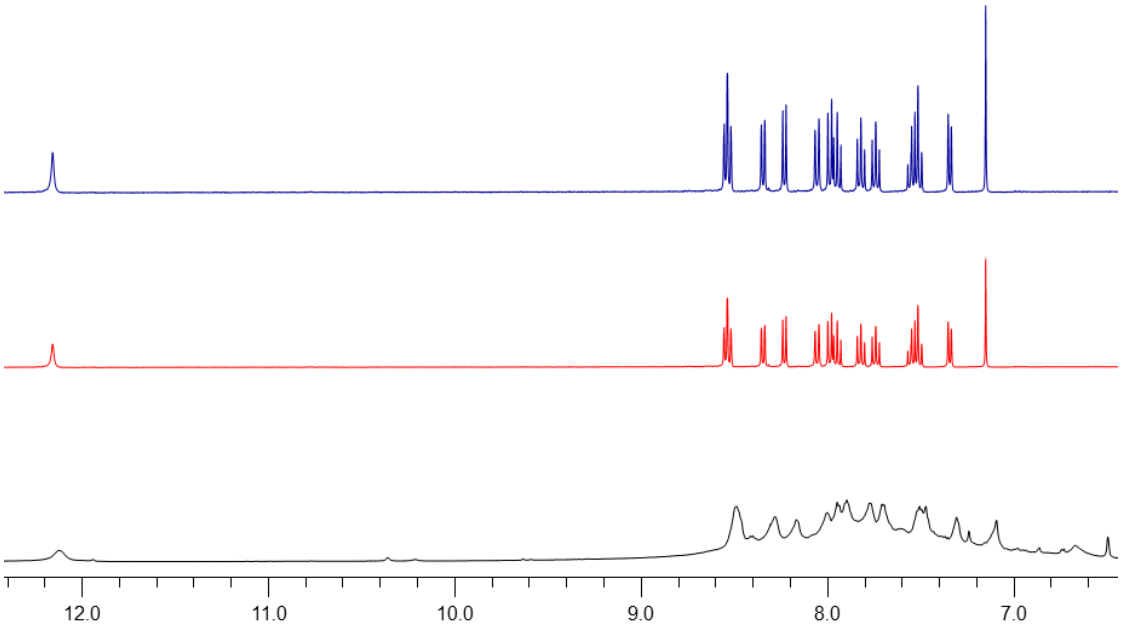

Fig. S3 ^{1}H NMR (400 MHz, 295 K) spectra of PNI in DMSO-d_6 at various concentration. c ≈ 2.9 mmolL^{-1} (blue), ≈ 9.0 mmolL^{-1} (red), ≈ 20 mmolL^{-1} (black).

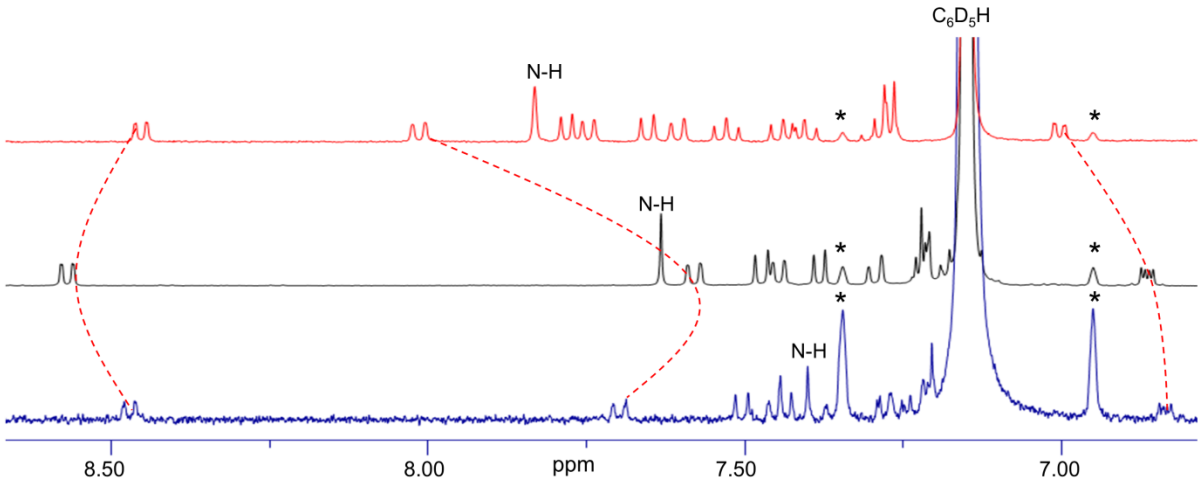

Fig. S4 ^{1}H NMR (400 MHz, 295 K) spectra of PNI in C_6D_6 (black), THF/C_6D_6 (red) and *n*-hexane/C_6D_6 (blue); satellite peaks are marked with asterisks.

4. IR spectroscopy

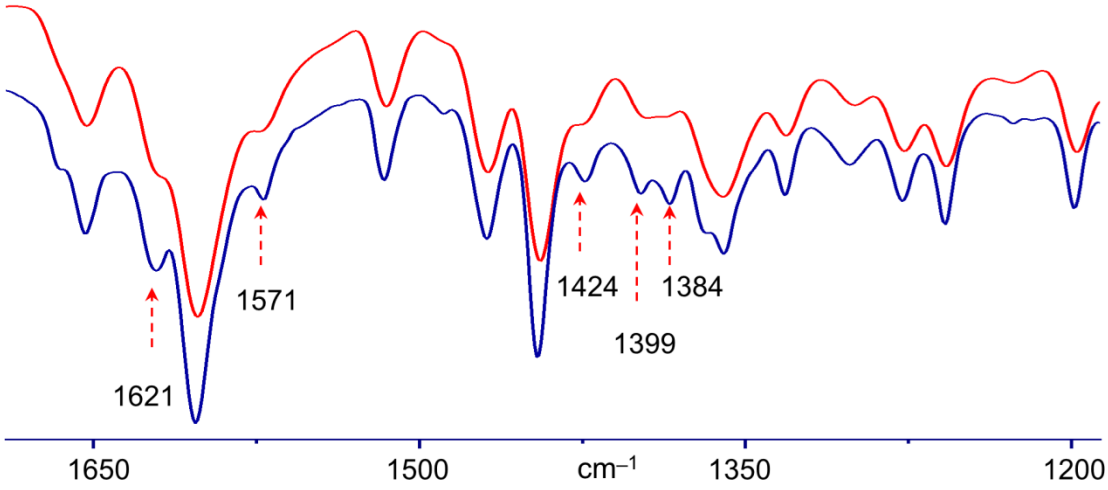

Fig. S5 Partial IR (KBr) spectra of monomeric (red) and aggregated (blue) PNI. The monomeric and the aggregated solid of PNI were prepared by room temperature evaporation of solution of the dye in THF and in mixture of THF/*n*-hexane (v/v = 1:9) respectively.

5. Powder XRD

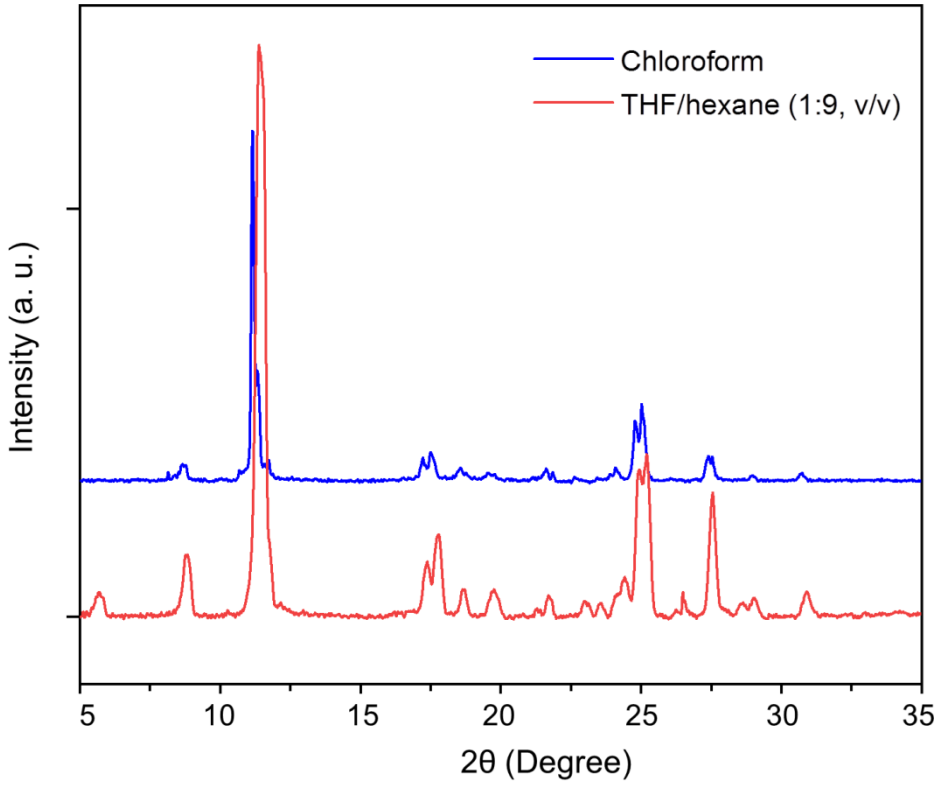

Fig. S6 Powder x-ray diffraction (XRD) patterns of bulk solid (blue) and self-assembled solid (red). Samples were prepared by evaporating PNI from chloroform and THF/*n*-hexane (v/v = 1/9) respectively

6. UV-vis spectroscopy

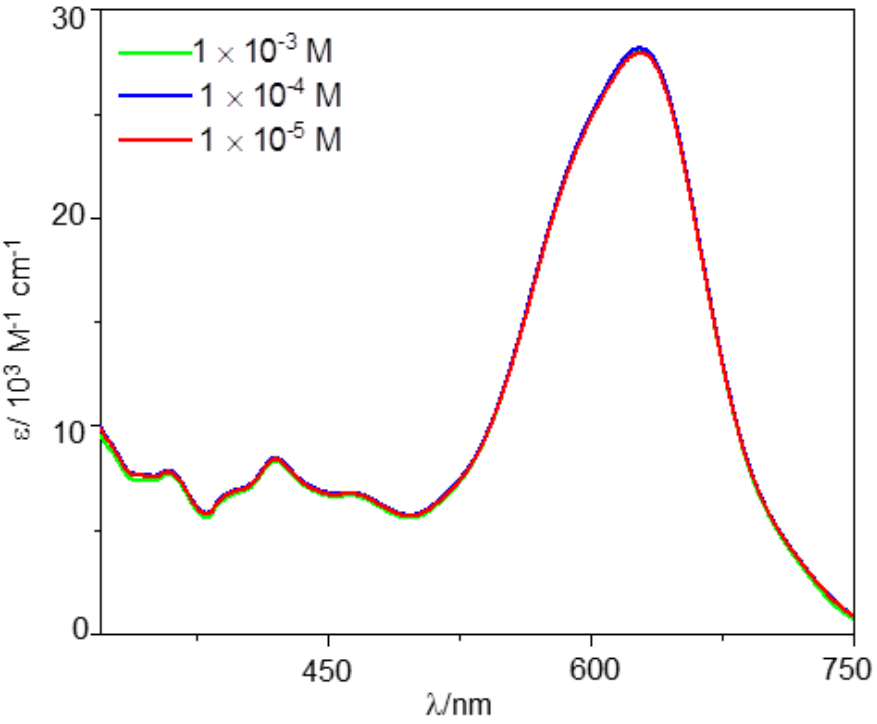

Fig. S7 Absorption spectra (293 K) of PNI in DMSO at various concentrations.

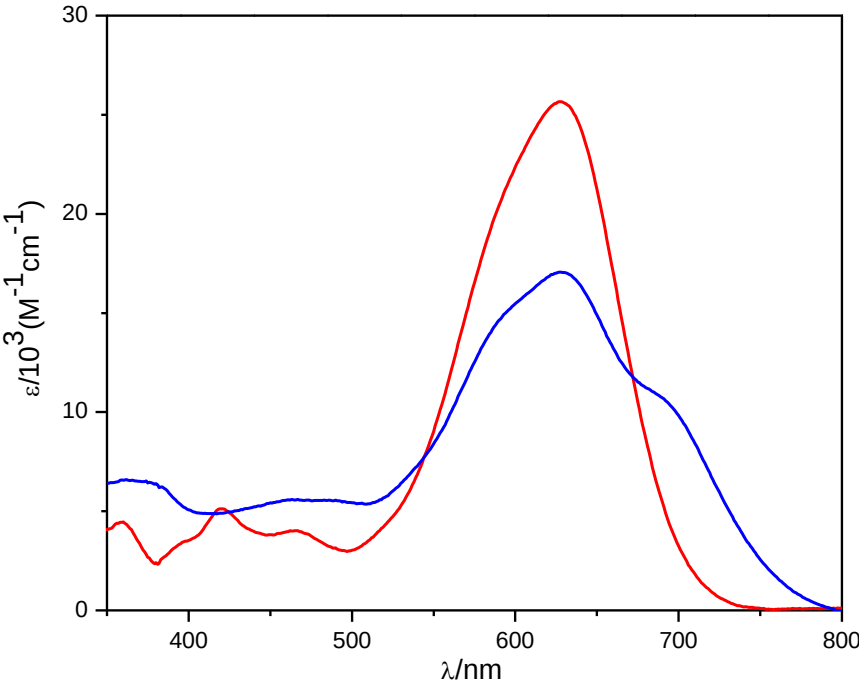

Fig. S8 Absorption spectra (293 K) of PNI ($c \approx 5 \times 10^{-6}$ $molL^{-1}$) in DMSO (red) and in mixture (blue) DMSO-water (v/v = 1:9).

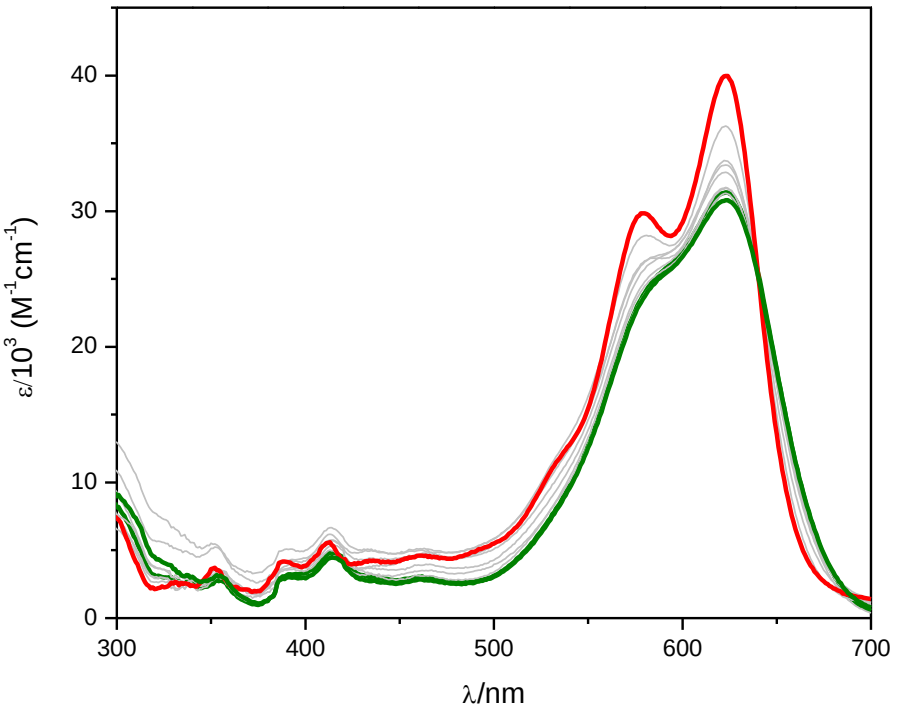

Fig. S9 Absorption spectra (293 K) of PNI (c ≈ 3 × 10^{-6} molL^{-1}) in THF (olive) and in mixture (red) of THF/*n*-hexane (v/v = 1:9). Spectra in grey colour are associated with intermediate fraction of *n*-hexane.

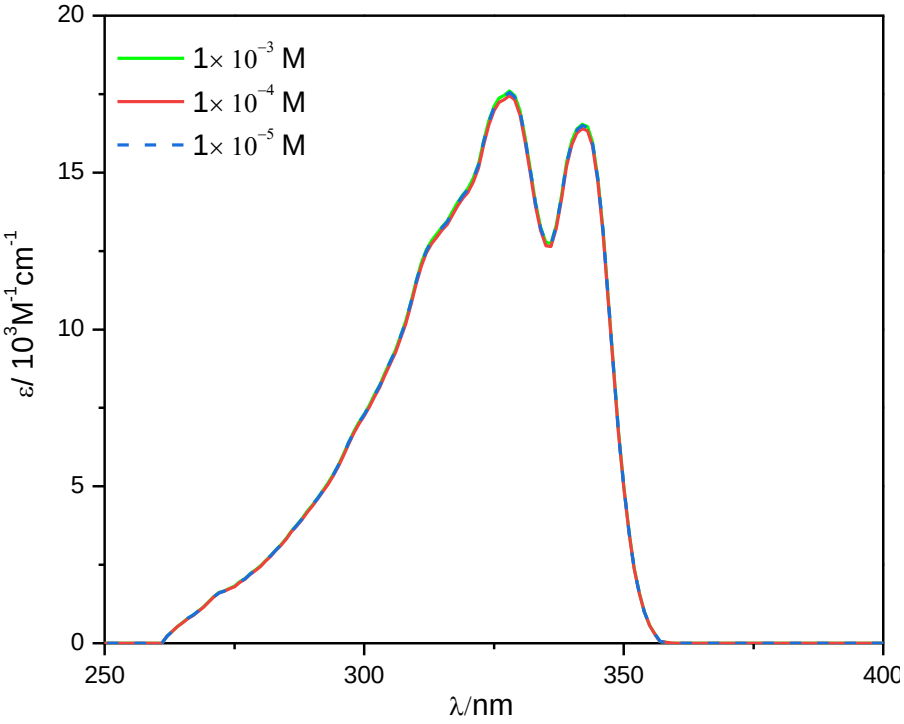

Fig. S10 Absorption spectra (293 K) of H-NMI at various concentrations in THF/*n*-hexane (v/v = 1:9) mixture.

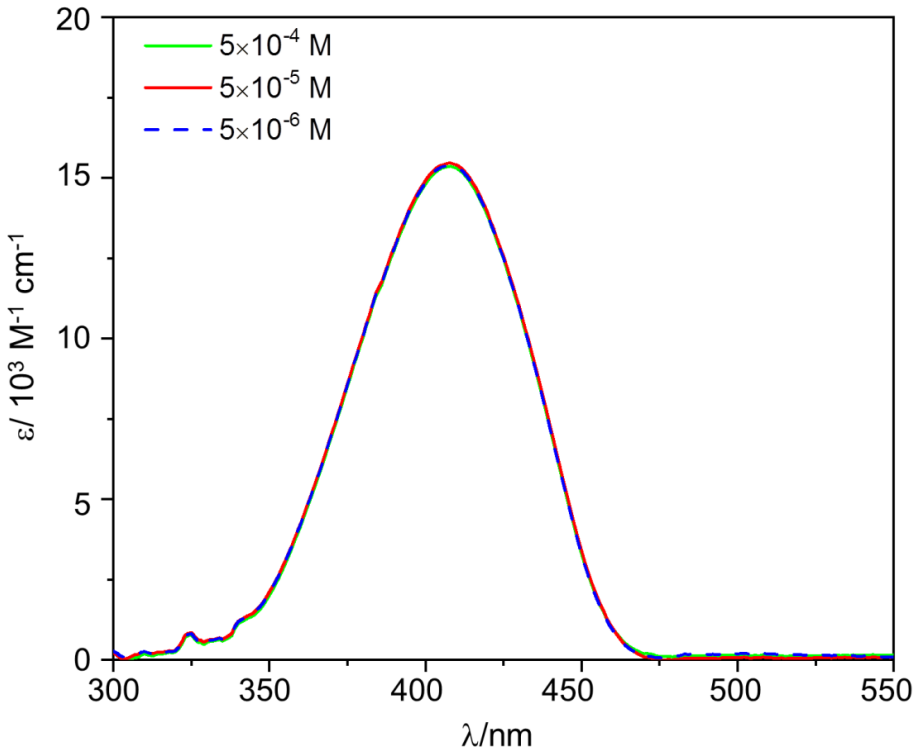

Fig. S11 Absorption spectra (293 K) of NH_2-NMI at various concentrations in THF/*n*-hexane (v/v =1:9) mixture.

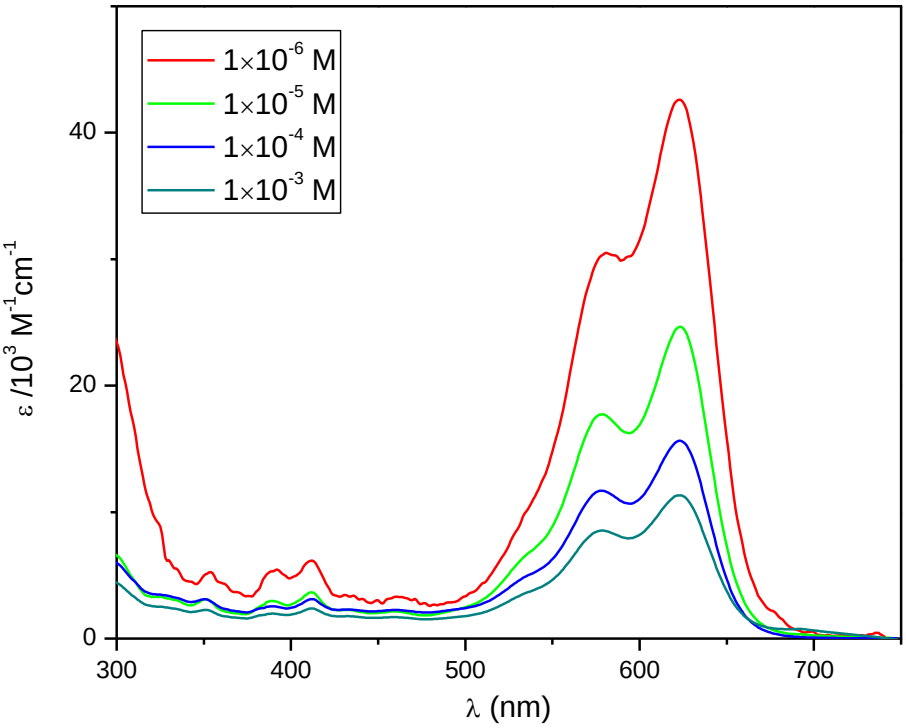

Fig. S 12 Absorption spectra (293 K) of PNI at various concentrations in THF/*n*-hexane (v/v =1:9) mixture. With increase in concentration the molar extinction co-efficient decreased, suggesting the formation of larger aggregates.

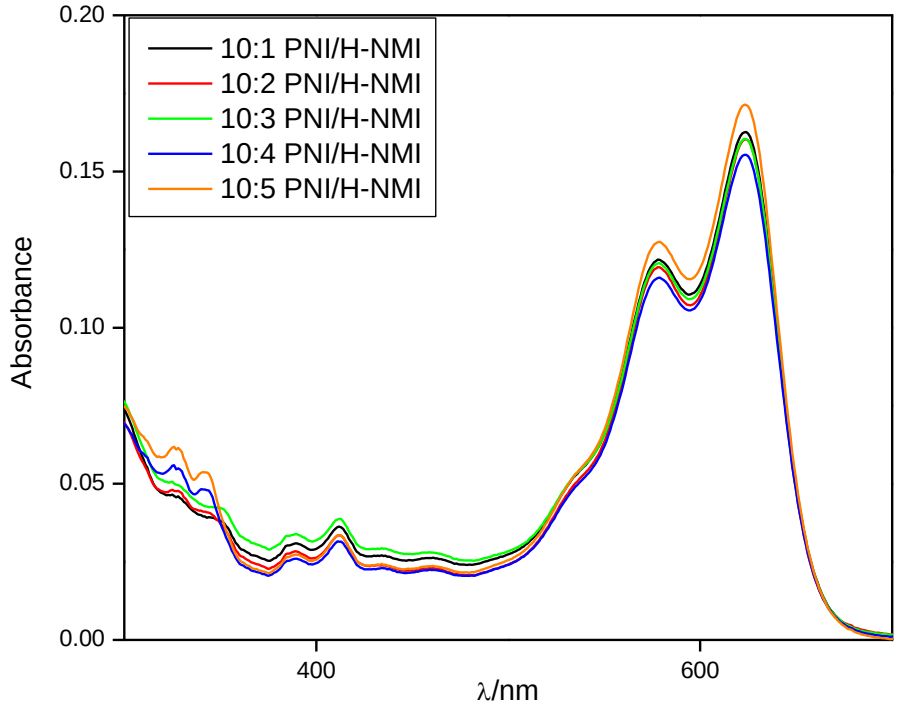

Fig. S13 Absorption spectra (293 K) of heteromeric aggregates of PNI and H-NMI in THF/*n*-hexane (v/v = 1:9) mixture. All measurements were done by mixing 3 x 10^{-6} $molL^{-1}$ of PNI with appropriate amounts of the H-NMI. The overall spectral changes were not additive with the increase in molar ratio of H-NMI in the co-self-assembly process. The spectral characteristic confirmed interactions of PNI with H-NMI.

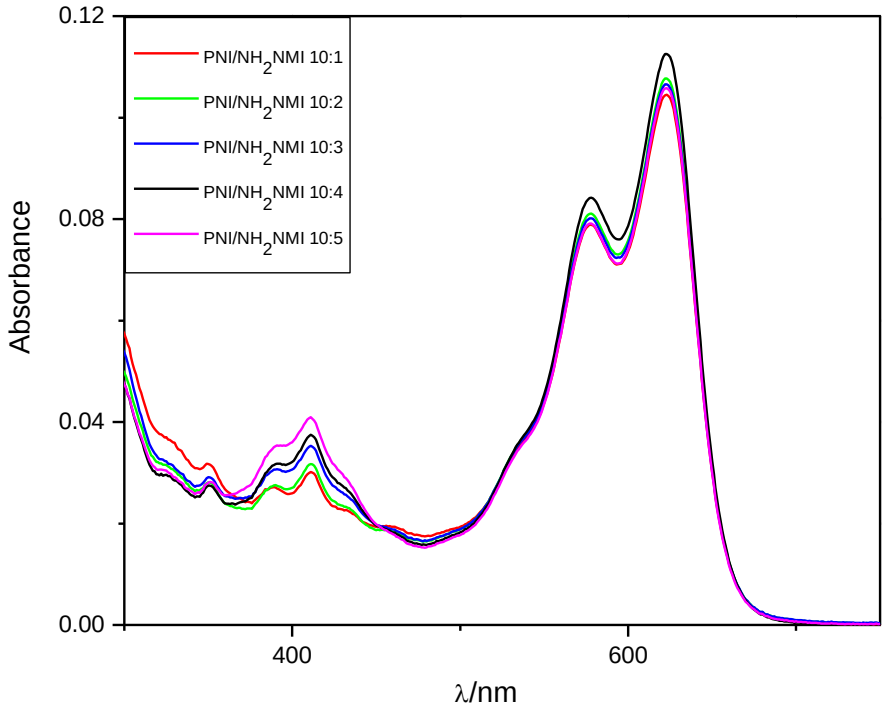

Fig. S14 Absorption spectra (293 K) of heteromeric aggregates of PNI and NH_2-NMI in THF/*n*-hexane (v/v = 1:9) mixture. All measurements were done by mixing 2.7 x 10^{-6} $molL^{-1}$ of PNI with appropriate amounts of the NH_2-NMI. The overall spectral changes were not additive with the increase in molar ratio of NH_2-NMI in the co-self-assembly process. The spectral characteristic confirmed interactions of PNI with NH_2-NMI.

7. Photoluminescence spectroscopy

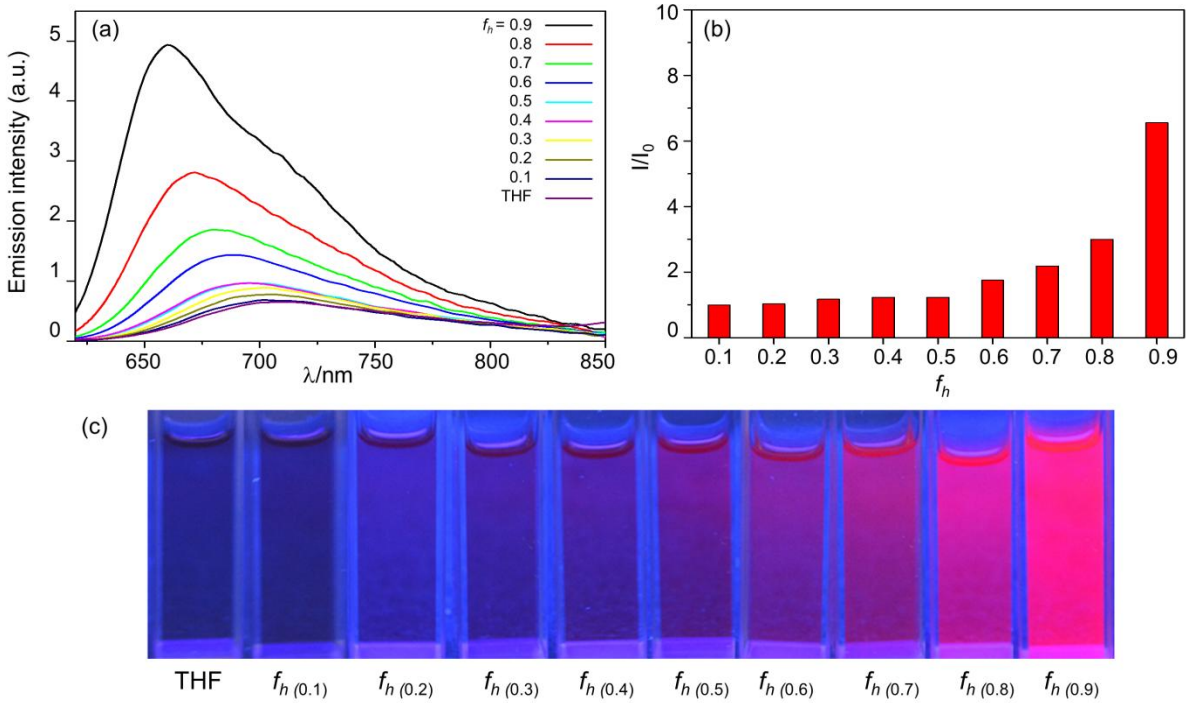

Fig. S15 (a) Photoluminescence spectra (293 K) of PNI (c ≈ 3 x 10^{-6} molL^{-1}) in THF and in mixture of THF/*n*-hexane. Spectra were recorded after excitation at 610 nm. (b) Photoluminescence enhancement of PNI with increase in fraction of *n*-hexane (f_h). The photoluminescence enhancement at various f_h were calculated by using the formula, $I/I_0 = \Phi_{fh}/\Phi_{THF}$. (c) Digital photograph of solution of PNI in THF and in different f_h. The photograph was captured after excitation with 365 nm UV lamp.

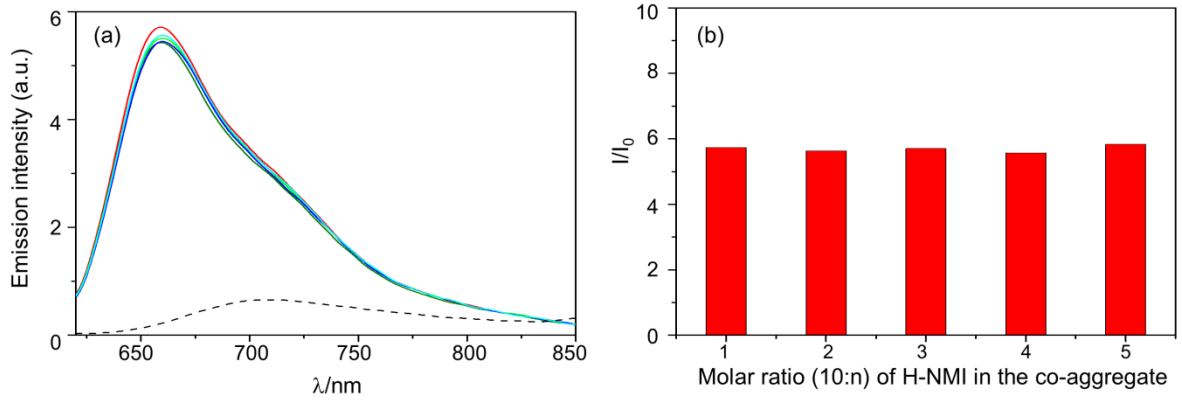

Fig. S16 (a) Photoluminescence spectra (293 K) of monomeric PNI (black dash) in THF and aggregated PNI (coloured) in the co-self-assembly with H-NMI in THF/*n*-hexane (v/v = 1:9). Co-aggregates were prepared by mixing PNI and H-NMI in 10: n (n= 1,2…5) molar ratio. Spectra were recorded after excitation at 610 nm and in all measurements concentration of PNI was kept same (c ≈ 3 × 10^{-6} molL^{-1}). (b) Photoluminescence enhancement of PNI in the co-aggregate with H-NMI at different molar ratio of the imide.

The Photoluminescence enhancement, $I/I_0 = (F^{fh}/F^{THF})(\eta_{fh}^2/\eta_{THF}^2)$.

Where F^{fh} and F^{THF} are the integrated intensities (areas) in heteromeric aggregate and in monomeric form, respectively; η_{fh} and η_{THF} are refractive indices of the respective solvents.

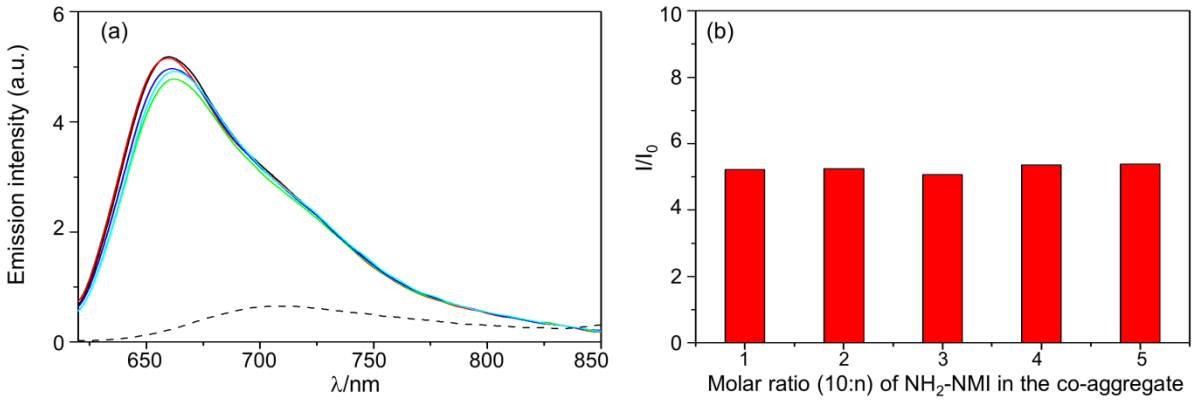

Fig. S17 (a) Photoluminescence spectra (293 K) of monomeric PNI (black dash) in THF and aggregated PNI (coloured solid) in the co-self-assembly with NH_2-NMI in THF/*n*-hexane (v/v = 1:9). Co-aggregates were prepared by mixing PNI and NH_2-NMI in 10: n (n= 1,2…5) molar ratio. Spectra were recorded after excitation at 610 nm, and in all measurements concentration of PNI was kept same ($c \approx 2.7 \times 10^{-6}$ $molL^{-1}$). (b) Photoluminescence enhancement of PNI in the co-aggregate with NH_2-NMI at different molar ratio of the imide.

The Photoluminescence enhancement, $I/I_0 = (F^{fh}/F^{THF})(\eta_{fh}^2/\eta_{THF}^2)$.

Where F^{fh} and F^{THF} are the integrated intensities (areas) in heteromeric aggregate and in monomeric form, respectively; η_{fh} and η_{THF} are refractive indices of the respective solvents.

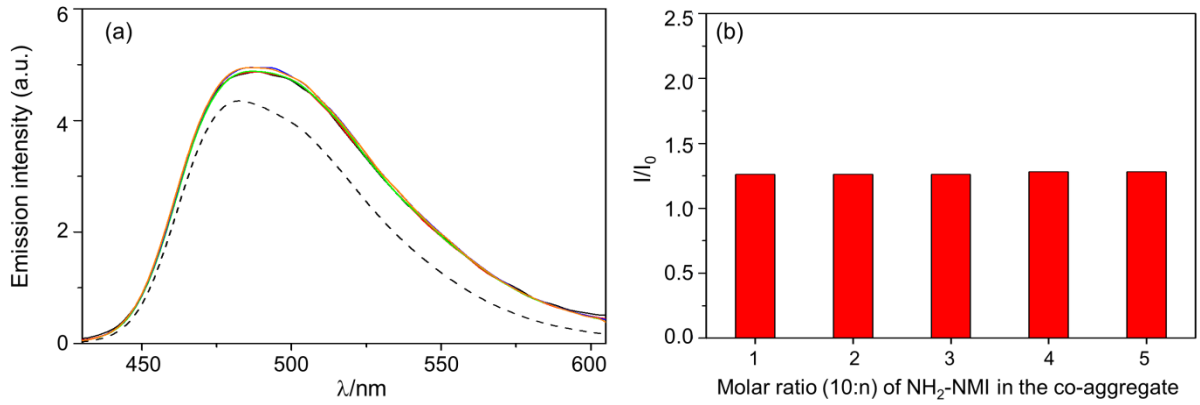

Fig. S18 (a) Photoluminescence spectra (293 K) of NH_2-NMI as monomer (black dash) and as co-aggregate with PNI (coloured) in THF/*n*-hexane (v/v = 1:9). Co-aggregates were prepared by mixing PNI and NH_2-NMI in 10: n (n= 1,2…5) molar ratio. Spectra were recorded after excitation at 410 nm. For comparison, spectra were divided by appropriate factors to keep NH_2-NMI concentration same. (b) Photoluminescence enhancement of NH_2-NMI in the co-aggregate with PNI at different molar ratio of the imide.

The Photoluminescence enhancement, $I/I_0 = (F^{co\text{-}aggregate}/F^{monomer})$.

$F^{co\text{-}aggregate}$ and $F^{monomer}$ are the integrated intensities (areas) in the heteromeric aggregate and in the monomeric form, respectively.

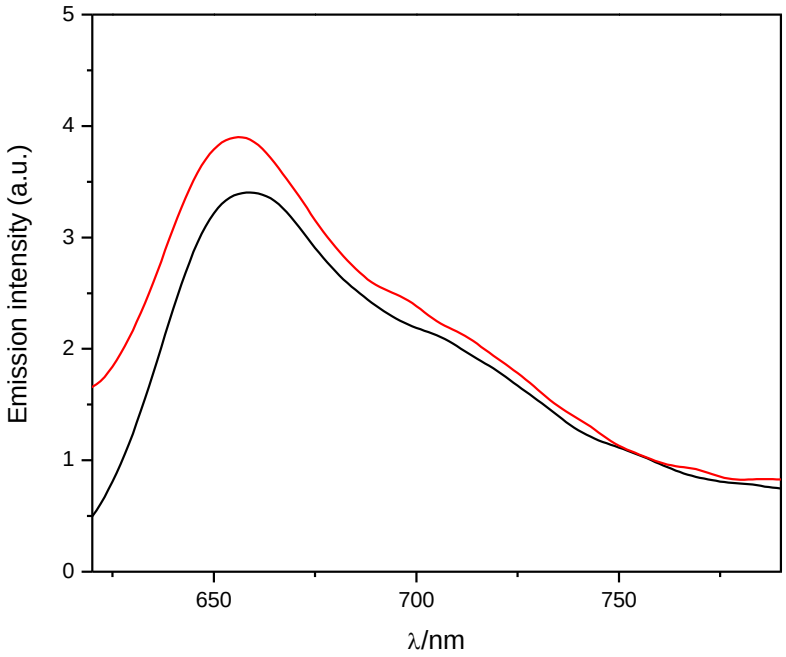

Fig. S19 (a) Photoluminescence spectra (293 K) of PNI in the heteromeric aggregate (red, PNI/NH_2-NMI 10:4) and in the homomeric aggregate (black) in THF/*n*-hexane (v/v = 1:9). Spectra were recorded after excitation at 410 nm. In both measurements concentration of PNI was kept same (c ≈ 2.7×10^{-6} $molL^{-1}$). The enhancement in emission was observed due to FRET process.

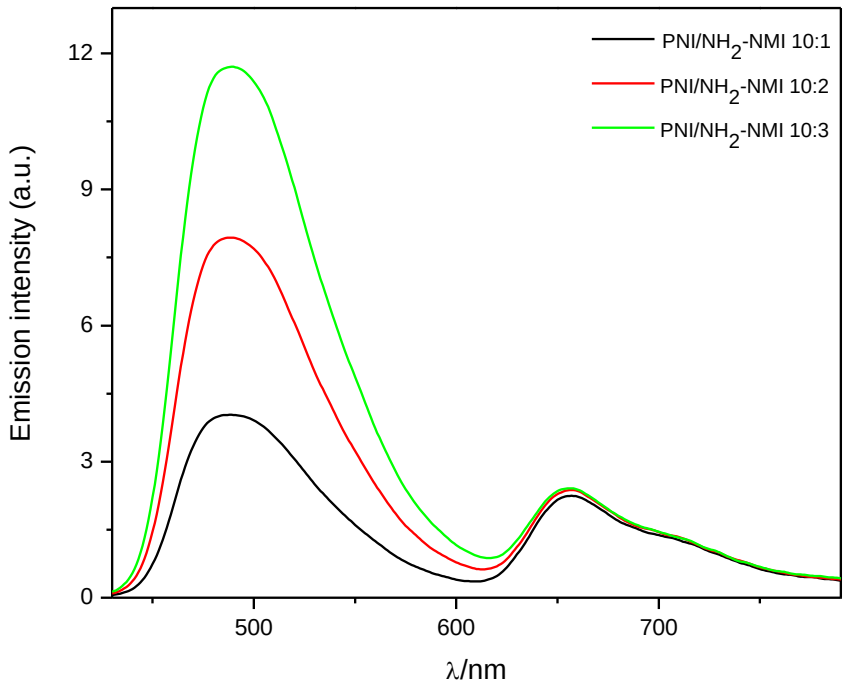

Fig. S20 (a) Photoluminescence spectra (293 K) of co-aggregates of PNI and NH_2-NMI in THF/*n*-hexane (v/v = 1:9). Co-aggregates were prepared by mixing PNI and NH_2-NMI in 10: n (n= 1, 2, 3) molar ratio. Spectra were recorded after excitation at 410 nm. In all measurements concentration of PNI was kept same (c ≈ 2.7×10^{-6} $molL^{-1}$).

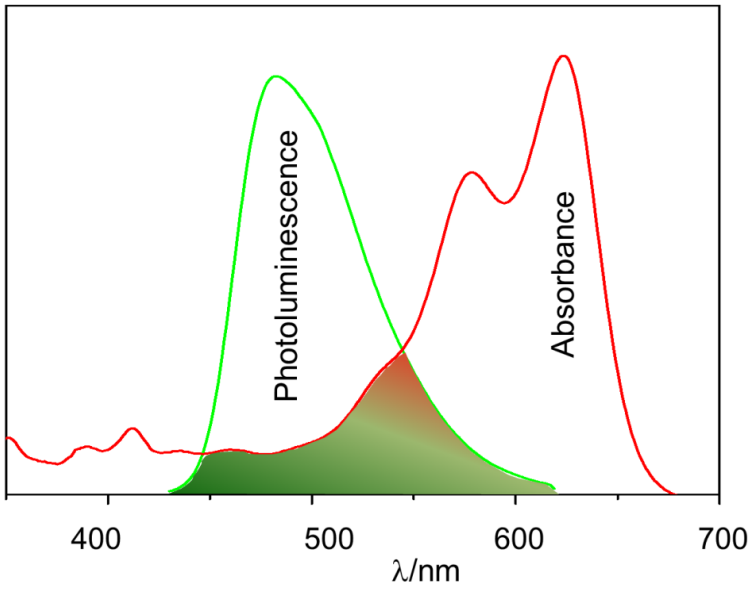

Fig. S21 (a) Spectral overlap between the emission of NH_2-NMI and the absorption of PNI.

8. FESEM images

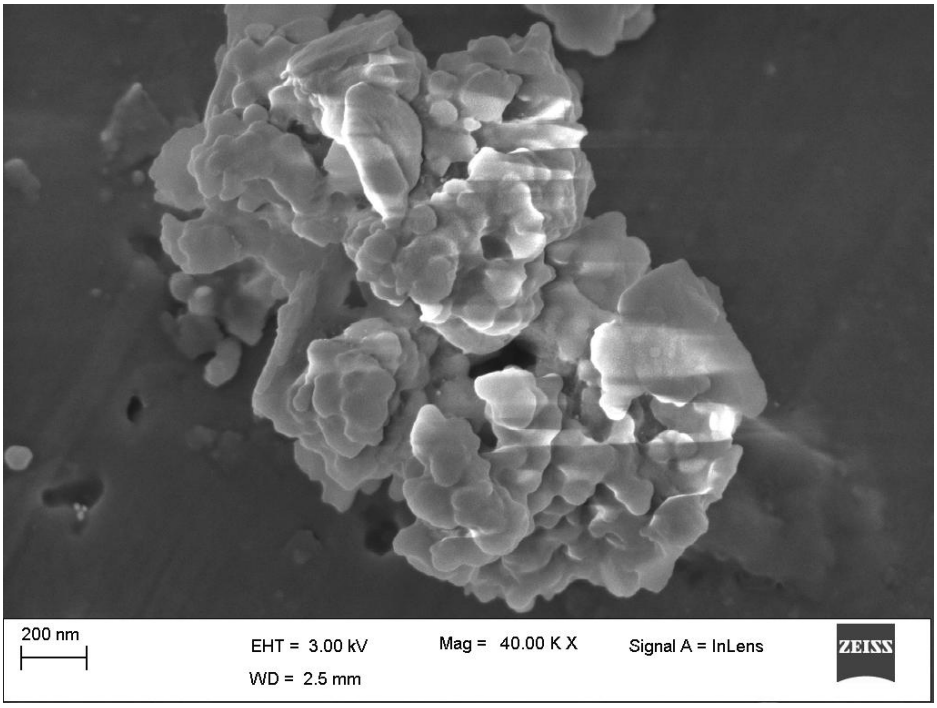

Fig. S22 FESEM image of aggregate of PNI in DMSO/water (v/v = 1:9). Image was captured after drop-casting a solution of the aggregate.

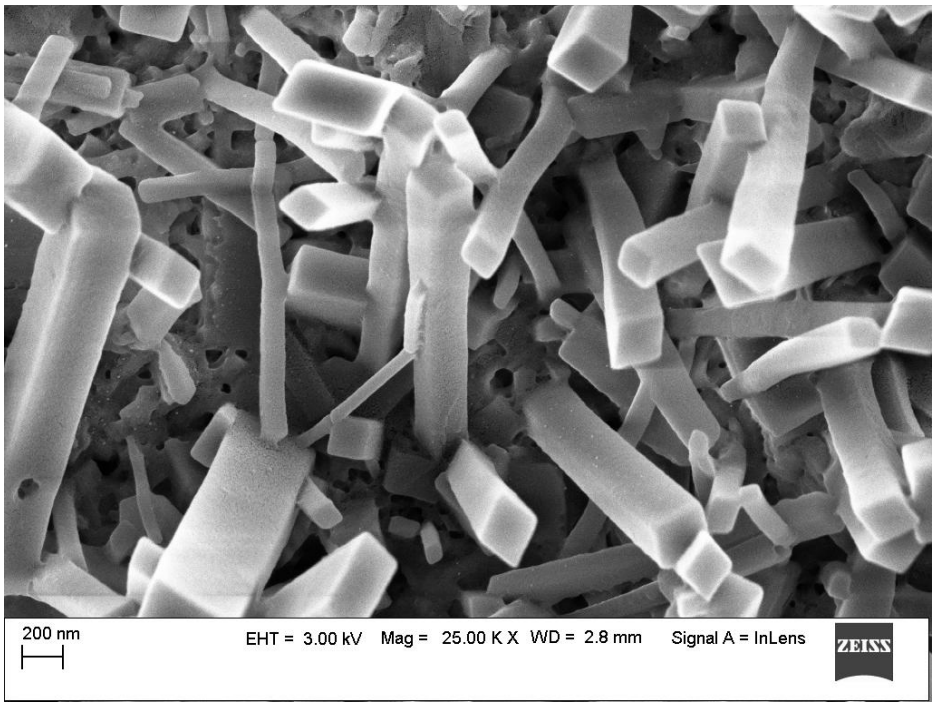

Fig. S23 FESEM image of aggregate of PNI in THF/*n*-hexane (v/v = 1:9). Image was captured after drop-casting a solution of the aggregate.

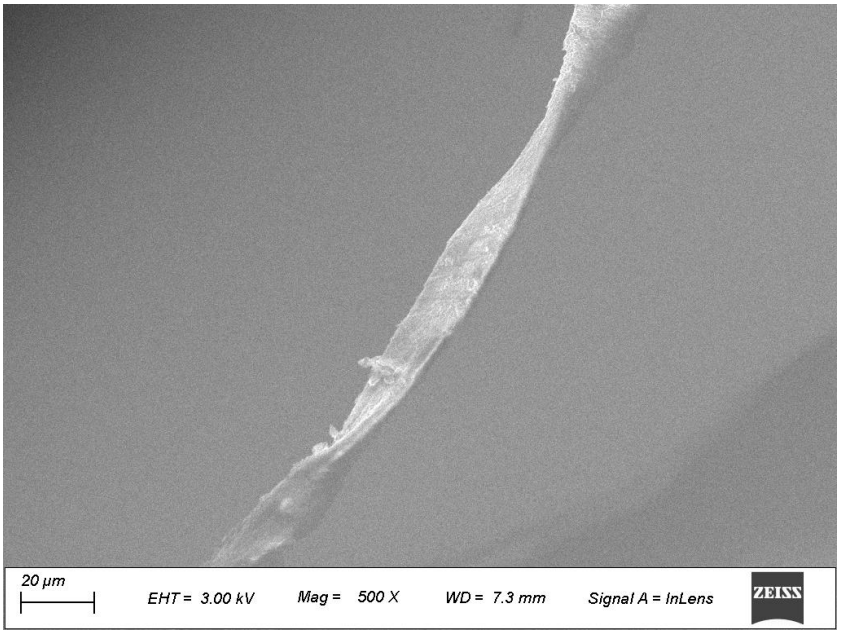

Fig. S24 FESEM image of co-aggregate of PNI and H-NMI in THF/*n*-hexane (v/v = 1:9). Image was captured after drop-casting a solution of co-aggregate, prepared by mixing PNI and H-NMI in 10: 2 molar ratio.

Fig. S25 FESEM image of co-aggregate of PNI and NH_2-NMI in THF/*n*-hexane (v/v = 1:9). Image was captured after drop-casting a solution of co-aggregate, prepared by mixing PNI and NH_2-NMI in 10:1 molar ratio.

9. Model for self-assembly and co-self-assembly processes

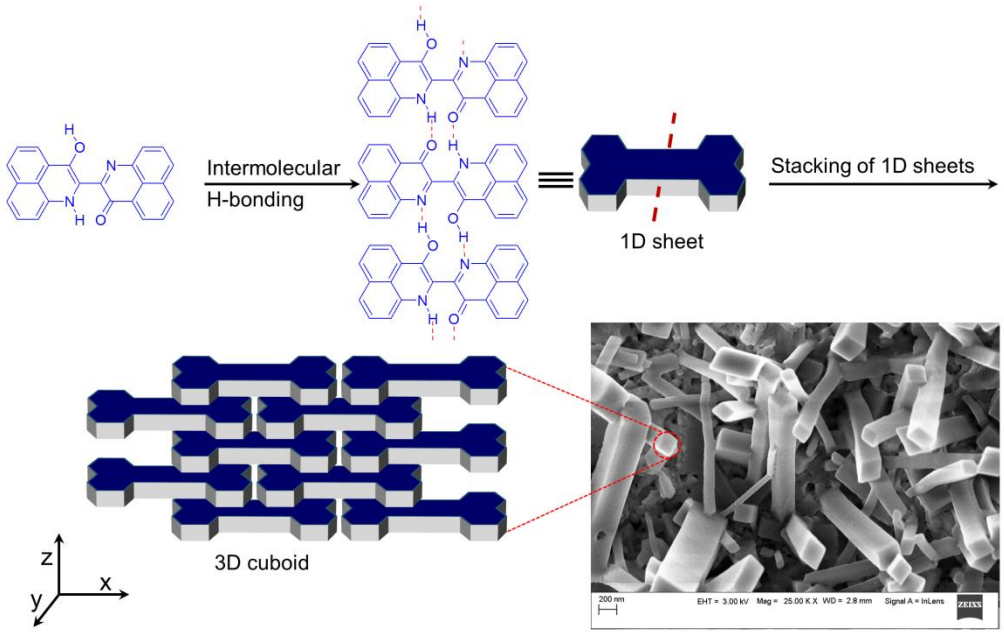

Fig. S26 Self-assembly process of PNI via intermolecular H-bonding followed by brick-wall type stacking. Intermolecular H-bonding provided growth in y-direction, while growth in x and z-direction was caused by brick wall type stacking.

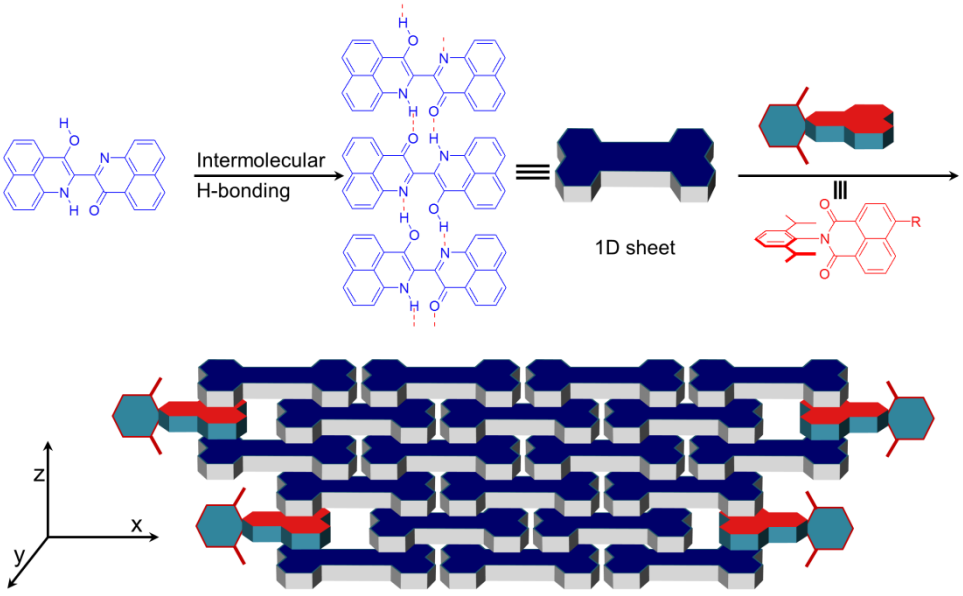

Fig. S27 Co-self-assembly process of PNI and 1,8-substituted naphthalimide derivatives. Sandwiching of imide in between PNI caused restricted growth in x-direction, leading to ribbon-shaped aggregate.

10. References

(1) R. J. Das and K. Mahata, *Org. Lett.*, 2018, **20**, 5027-5031.
(2) T. Weil, E. Reuther and K, Müllen, *Angew. Chem., Int. Ed.* 2002, **41**, 1900-1904.
(3) A. Boehm, H. Schmeisser, S. Becker and K. Mullen, *Ger. Offen.*, 2001, DE 19940708 A120010301.